On Periodic Control Laws for Mobile Robots

Sašo Blažič

***Abstract*—This paper deals with the control of differentially driven wheeled mobile robots. Two families of wheeled mobile robots are considered: those that are capable of forward motion only and those that can perform forward and backward motion. A unified framework for the control law analysis and design of both robot types is proposed. The control laws are developed within a Lyapunov stability analysis framework. Periodic Lyapunov functions are proposed, and the constructive procedure leads to periodic control laws. These laws are very natural for wheeled mobile robots since they are inspired by the periodic nature of a robot's orientation. The simple form of the control laws enables their easy implementation in practical applications. Global convergence is proven based on the usual requirements for reference velocities. Some important properties of these systems are also treated, such as continuity and the presence of unstable equilibria. Some guidelines for how to choose a suitable control law and its parameters are also given. An extensive simulation study was performed, and the results of the proposed control laws are compared with some control laws from the literature. The algorithms were also validated using the Mirosot-type robot soccer robot and a vision-based system.**

***Index Terms*—Error model, kinematic model, Lyapunov stability analysis, periodic control law, trajectory tracking, wheeled mobile robot.**

I. Introduction

AUTONOMOUS mobile robots have become very popular in recent years. The number of industrial applications and research publications is rapidly growing [1]–[5]. There are many issues to be solved when designing a mobile robot system. Among them, the problem of nonholonomic system control plays an important role. A thoroughly studied case with great practical significance is the wheeled mobile robot with a kinematic model similar to a unicycle. The differentially driven mobile robots that are very common in practical applications also have such a kinematic model. Although many researchers coped with the more difficult problem of stabilizing dynamic models for different types of mobile robots (see, e.g., [6]), the basic limitations of mobile robot control still come from their kinematic model, as shown in [7]–[9]. Kinematic control laws are also very important from the practical point of view since the wheel velocity control is often locally implemented on simple microcontroller-based hardware, whereas the velocity command comes from high-level hardware, which also provides the current control objective.

Manuscript received October 10, 2012; revised February 7, 2013, April 29, 2013, and July 22, 2013; accepted October 7, 2013. Date of publication October 24, 2013; date of current version January 31, 2014.

The author is with the Faculty of Electrical Engineering, University of Ljubljana, 1000 Ljubljana, Slovenia (e-mail: saso.blazic@fe.uni-lj.si).

Color versions of one or more of the figures in this paper are available online at http://ieeexplore.ieee.org.

Digital Object Identifier 10.1109/TIE.2013.2287222

Traditionally, the problem of mobile robot control has been approached using point stabilization [10] or by redefining the problem as a tracking control one [11]. There are also some approaches that tackle both problems simultaneously [2]. However, in our opinion, the tracking control approach is somewhat more appropriate since the nonholonomic constraints and other control goals (obstacle avoidance, minimum travel time, minimum fuel consumption) are implicitly included in the path-planning procedure [12]. It is also easier to extend this approach to more complex schemes such as the control of mobile robot platoons [13]. Many control algorithms were proposed in the path-tracking framework, such as proportional–integral–differential (PID) controllers [11], Lyapunov-based nonlinear controllers [14], [15], adaptive controllers [6], model-based predictive controllers [16], fuzzy-systems-based controllers [17], [18], visual servoing controllers [19], [20], etc. In some cases, they are implemented on chips or other industrial hardware [21]. Some approaches only guarantee local stability, whereas others also ensure global stability and global convergence under certain assumptions.

In this paper, a very important property of mobile robot systems is treated. The model of a wheeled mobile robot can be seen as being periodic with respect to its orientation. This property of the system should be also reflected in the control law. However, it has not often been explicitly treated, although some control laws that belong to the group of periodic control laws exist [11]. Some geometrically inspired control laws resemble the laws treated in this paper, e.g., pure-pursuit path tracking [22]. In this paper, a wide spectrum of periodic control laws is developed. Forward-motion-only control is treated first, and later, a generalization to forward and backward motion control is introduced. The latter group of mobile robots has not been often explicitly treated in the literature. All the laws are derived within the Lyapunov stability framework. The control laws are also discussed from the continuity point of view. On one hand, it is very important to find a (kinematic) control law that produces a smooth control signal. If this is not the case, the implementation on the dynamic model becomes difficult due to a discontinuity in the orientation error of $\pm 180^\circ$, which often leads to a discontinuity in the angular velocity command. On the other hand, continuous control laws often suffer from an unstable equilibrium at a certain orientation error. The tradeoff between these two important system properties will be also discussed. Last but not the least, the proposed control laws are very easy to implement since they are mostly composed of trigonometric functions.

The problem statement is given in Section II. The Lyapunov-functions-based control design is described in Section III. In Section IV, several control algorithms are compared. Practical

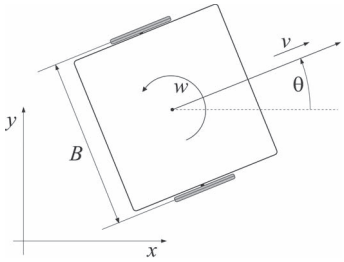

Fig. 1. Two-wheeled differentially driven mobile robot.

experiments are described in Section V. The conclusions are stated in Section VI.

II. Problem Statement

Assume a two-wheeled differentially driven mobile robot like the one depicted in Fig. 1, where (x, y) is the wheel axis center position, and θ is the robot orientation. The kinematic motion equations of such a mobile robot are equivalent to those of a unicycle. Robots with such an architecture have a nonholonomic constraint of the form

$$[-\sin\theta(t) \quad \cos\theta(t)] \begin{bmatrix} \dot{x}(t) \\ \dot{y}(t) \end{bmatrix} = 0 \tag{1}$$

resulting from the assumption that the robot cannot move in the lateral direction. Only the first-order kinematic model of the system will be treated in this paper, i.e.,

$$\dot{q} = \begin{bmatrix} \dot{x} \\ \dot{y} \\ \dot{\theta} \end{bmatrix} = \begin{bmatrix} \cos\theta & 0 \\ \sin\theta & 0 \\ 0 & 1 \end{bmatrix} \begin{bmatrix} v \\ w \end{bmatrix} \tag{2}$$

where $q^T(t) = [x(t) \quad y(t) \quad \theta(t)]$ is the vector of generalized coordinates, whereas v and w are the translational and angular velocities, respectively, of the system in Fig. 1. The velocities of the right and left wheels of the robot are

$$v_R = v + \frac{wB}{2} \quad \text{and} \quad v_L = v - \frac{wB}{2} \tag{3}$$

where B is the robot interwheel distance. The control design goal is to follow the reference trajectory, which is defined by

$$q_r^T(t) = [x_r(t) \quad y_r(t) \quad \theta_r(t)] \tag{4}$$

where $q_r(t)$ is *a priori* known and smooth. It is very easy to show that the system (2) is flat, with the flat outputs being x and y. This flatness property guarantees the existence of the uniformly continuous control inputs $v_r(t)$ and $w_r(t)$ that produce the desired trajectory (4) in the ideal case of the kinematic constraints described by (1) if a condition on the nonzero translational velocity is met at each moment of time. For a given smooth reference trajectory (4) defined in the time interval $t \in [T_s, T_f]$, the open-loop (or flatness-based) control can be derived as

$$\begin{aligned} v_r(t) &= \sqrt{\dot{x}_r^2(t) + \dot{y}_r^2(t)} \\ w_r(t) &= \frac{\dot{x}_r(t)\ddot{y}_r(t) - \dot{y}_r(t)\ddot{x}_r(t)}{\dot{x}_r^2(t) + \dot{y}_r^2(t)} \\ &= v_r(t)\kappa(t) \end{aligned} \tag{5}$$

where $\kappa(t)$ is the reference path's curvature. The necessary condition for the existence of (5) is a twice-differentiable path and a nonzero tangential velocity $v_r(t) \neq 0, \forall\, t \in [T_s, T_f]$.

The posture error is not given in the global coordinate system but rather as an error in the local coordinate system of the robot: e_x gives the error in the direction of driving, e_y gives the error in the lateral direction, and e_θ gives the error in the orientation. The posture error $e = [\, e_x \quad e_y \quad e_\theta \,]^T$ is determined using the actual posture $q = [\, x \quad y \quad \theta \,]^T$ and the reference posture $q_r = [\, x_r \quad y_r \quad \theta_r \,]^T$, i.e.,

$$\begin{bmatrix} e_x \\ e_y \\ e_\theta \end{bmatrix} = \begin{bmatrix} \cos\theta & \sin\theta & 0 \\ -\sin\theta & \cos\theta & 0 \\ 0 & 0 & 1 \end{bmatrix} (q_r - q). \tag{6}$$

From (2) and (6) and assuming that the virtual reference robot has a kinematic model similar to (2), the posture error model can be written as follows:

$$\begin{bmatrix} \dot{e}_x \\ \dot{e}_y \\ \dot{e}_\theta \end{bmatrix} = \begin{bmatrix} \cos e_\theta & 0 \\ \sin e_\theta & 0 \\ 0 & 1 \end{bmatrix} \begin{bmatrix} v_r \\ w_r \end{bmatrix} + \begin{bmatrix} -1 & e_y \\ 0 & -e_x \\ 0 & -1 \end{bmatrix} u. \tag{7}$$

The transformation (6) is theoretically imposed by the group operation, noting that the model (2) is a system in the Lie group SE(2) [8]. This approach was adopted in [11], where the authors also proposed PID control for the stabilization of the robot at the reference posture. Later, many authors used the error model (7) for the tracking control design.

Very often, e.g., [11], the control u is used to solve the tracking problem, i.e.,

$$u = \begin{bmatrix} v \\ w \end{bmatrix} = \begin{bmatrix} v_r \cos e_\theta + v_b \\ w_r + w_b \end{bmatrix} \tag{8}$$

where $u_b^T = [\, v_b \quad w_b \,]$ is the feedback signal to be determined later. Inserting the control (8) into (7), the resulting error model is given by

$$\begin{aligned} \dot{e}_x &= w_r e_y - v_b + e_y w_b \\ \dot{e}_y &= -w_r e_x + v_r \sin e_\theta - e_x w_b \\ \dot{e}_\theta &= -w_b. \end{aligned} \tag{9}$$

The goal of this paper is to design a feedback tracking controller, and the tracking should be asymptotic under the persistency of excitation through $v_r(t)$ or $w_r(t)$. The control laws will be periodic with respect to the orientation error. Thus, all the usual problems with orientation are alleviated. These problems can become critical around $\pm 180^\circ$ in certain applications, e.g., when using an observer to estimate the robot pose from the delayed measurements.

Two types of wheeled mobile robots will be treated in this work. The first group consists of mobile vehicles that can perform forward motion only. They can drive only in one direction during normal operation due to the fact that the service equipment is only mounted on one side of the vehicle in the direction of movement. Sometimes, reverse driving is allowed during special maneuvers, e.g., during the initial transient to approach the reference trajectory or during zigzag lateral

movement. The second group consists of mobile robots that are capable of forward and backward motion. Usually, they are (approximately) symmetric and can perform their tasks when driving in any of the two directions dictated by the nonholonomic constraints.

III. Periodic Control Laws for Wheeled Mobile Robots

The problem of tracking is clearly periodic with respect to the orientation. This can be observed from the kinematic model (2) by using an arbitrary control input and an arbitrary initial condition, resulting in a certain robot trajectory. If the same control input is applied to the robot and the initial condition only differs from the previous one by a multiple of 2π, the same response is obtained for $x(t)$ and $y(t)$, whereas $\theta(t)$ differs from the previous solution for the same multiple of 2π. The periodic nature should be also reflected in the control law used for the tracking. This should mean that one searches for a control law that is periodic with respect to the error in the orientation e_θ (the period is 2π) and ensures the convergence of the posture error e to one of the points $[\,0 \quad 0 \quad 2k\pi\,]^T$ $(k \in \mathbb{Z})$.

Obviously, the functions that are used in this paper for the convergence analysis should be also periodic in e_θ. This means that these functions have multiple local minima and therefore do not satisfy the properties of the classic Lyapunov functions. Although the stability analysis resembles Lyapunov's direct method (the second method of Lyapunov), the convergence is not proven by this stability theory because the convergence of e to zero is not needed in our approach. Nevertheless, the functions used in this paper for the convergence analysis will still be referred to as "Lyapunov functions."

In the stability proofs of the control laws in this paper, the signal norms will play an important role. The $\mathcal{L}_p$ norm of a scalar function $x(t)$ is defined as

$$\|x\|_p = \left(\int_0^\infty |x(\tau)|^p \, d\tau \right)^{\frac{1}{p}}. \tag{10}$$

If the preceding integral exists (i.e., it is finite), the function $x(t)$ is said to belong to $\mathcal{L}_p$. Limiting p toward infinity provides a very important class of functions, i.e., $\mathcal{L}_\infty$-bounded functions.

Two very well-known lemmas will be used in the proofs of the theorems in this paper. The first one is Barbãlat's lemma, and the other one is a derivation of Barbãlat's lemma. Both lemmas are taken from [23] and are given below for the sake of completeness.

Lemma 1 (Barbãlat's Lemma): If $\lim_{t\to\infty} \int_0^t f(\tau)d\tau$ exists and is finite and $f(t)$ is a uniformly continuous function, then $\lim_{t\to\infty} f(t) = 0$.

Lemma 2: If $f,\ \dot{f} \in \mathcal{L}_\infty$ and $f \in \mathcal{L}_p$ for some $p \in [1, \infty)$, then $f(t) \to 0$ as $t \to \infty$.

A. Forward Motion Control of Wheeled Mobile Robots

When controlling a vehicle that can perform forward motion only, our goal is to bring the position error to zero, whereas the orientation error should converge to any multiple of 2π. In order to do this, a Lyapunov function that is periodic with respect to e_θ (with a natural period of 2π) will be used. First, the concept will be shown on one Lyapunov function, and later, this will be extended to a more general case. The first Lyapunov function candidate is chosen as

$$V = \frac{k_y}{2}\left(e_x^2 + e_y^2\right) + \frac{1}{2}\left(\frac{\tan\frac{e_\theta}{2}}{\frac{1}{2}}\right)^2 \tag{11}$$

where k_y is a positive constant. Its derivative along the solutions of (9) is

$$\begin{aligned}\dot{V} &= k_y e_x(w_r e_y - v_b + e_y w_b) \\ &\quad + k_y e_y(-w_r e_x + v_r \sin e_\theta - e_x w_b) - 2\frac{\tan\frac{e_\theta}{2}}{\cos^2\frac{e_\theta}{2}} w_b \\ &= -k_y e_x v_b + k_y v_r e_y \sin e_\theta - 2\frac{\tan\frac{e_\theta}{2}}{\cos^2\frac{e_\theta}{2}} w_b \end{aligned} \tag{12}$$

if the following control law is applied:

$$\begin{aligned} v_b &= k_x e_x \\ w_b &= k_y v_r e_y \cos^4\frac{e_\theta}{2} + k_\theta \sin e_\theta \end{aligned} \tag{13}$$

where k_x and k_θ are positive bounded functions; the derivative $\dot{V}$ from (12) becomes

$$\dot{V} = -k_x k_y e_x^2 - k_\theta \left(\frac{\tan\frac{e_\theta}{2}}{\frac{1}{2}}\right)^2. \tag{14}$$

The asymptotic stability of the equilibrium points $e_k = [\,0 \quad 0 \quad 2k\pi\,]^T$ $(k \in \mathbb{Z})$ will be shown in Theorem 1.

Theorem 1: If the control law (13) is applied to the system where k_y is a positive constant, k_x and k_θ are positive bounded functions, the reference velocities v_r and w_r are bounded, and the initial condition for $e_\theta(t)$ satisfies $\cos(e_\theta(0)/2) \neq 0$, then the tracking error e_x converges to 0, whereas e_θ converges to a multiple of 2π. The convergence of e_y to 0 is guaranteed, provided that at least one of these two conditions is met:

1) v_r is uniformly continuous and does not go to 0 as $t \to \infty$, whereas k_θ is uniformly continuous;
2) w_r is uniformly continuous and does not go to 0 as $t \to \infty$, whereas v_r, k_x, and k_θ are uniformly continuous.

Proof: It follows from (14) that $\dot{V} \leq 0$, and therefore, the Lyapunov function is nonincreasing and thus has the limit $\lim_{t\to\infty} V(t)$. Consequently, the following can be concluded from (11):

$$e_x,\ e_y,\ \tan\frac{e_\theta}{2} \in \mathcal{L}_\infty. \tag{15}$$

Based on (15), it follows from (13) that the control signals are bounded and from (9) that the derivatives of the errors are bounded, i.e.,

$$v_b,\ w_b,\ \dot{e}_x,\ \dot{e}_y,\ \dot{e}_\theta \in \mathcal{L}_\infty \tag{16}$$

where it was taken into account that v_r, w_r, k_x, and k_θ are bounded.

In order to show the asymptotic stability of the equilibrium points, let us first calculate the following integral:

$$\int_0^\infty \dot{V}dt = V(\infty) - V(0) = -\int_0^\infty k_x k_y e_x^2 dt - 4\int_0^\infty k_\theta \tan^2\frac{e_\theta}{2}dt. \tag{17}$$

Since $V \geq 0$, the following inequality follows from (17):

$$\begin{aligned} V(0) &\geq \int_0^\infty k_x k_y e_x^2 dt + 4\int_0^\infty k_\theta \tan^2\frac{e_\theta}{2}dt \\ &\geq k_y \underline{k}_x \int_0^\infty e_x^2 dt + 4\underline{k}_\theta \int_0^\infty \tan^2\frac{e_\theta}{2}dt \end{aligned} \tag{18}$$

where the lower bounds of the functions $k_x(t)$ and $k_\theta(t)$ are introduced, i.e.,

$$\begin{aligned} k_x(t) &\geq \underline{k}_x > 0 \\ k_\theta(t) &\geq \underline{k}_\theta > 0. \end{aligned} \tag{19}$$

It follows from (18) that $e_x, \tan(e_\theta/2) \in \mathcal{L}_2$. Applying Lemma 2, the convergence of $e_x(t)$ to 0 immediately follows. Next, the convergence of $\tan(e_\theta/2)$ to 0 will be established. The function is bounded due to (15). It also belongs to $\mathcal{L}_2$, as shown above. It remains to be shown that $(d/dt)\tan(e_\theta/2) = (\cos(e_\theta/2))^{-2}(\dot{e}_\theta/2) \in \mathcal{L}_\infty$. The second factor is bounded [see (16)], whereas the first factor is also bounded by the initial value of the Lyapunov function

$$\left(\cos\frac{e_\theta}{2}\right)^{-2} = 1 + \tan^2\frac{e_\theta}{2} \leq 1 + \frac{V(t)}{2} \leq 1 + \frac{V(0)}{2}. \tag{20}$$

Since $\cos(e_\theta(0)/2) \neq 0$ from the assumption of the theorem (and therefore $V(0)$ is finite) and V is nonincreasing, $(\cos(e_\theta/2))^{-2}$, $(d/dt)\tan(e_\theta/2) \in \mathcal{L}_\infty$. Consequently, it follows from Lemma 2 that $\tan(e_\theta(t)/2) \to 0$ or, equivalently, $e_\theta(t) \to 2k\pi$ $(k \in \mathbb{Z})$. Since the limit $\lim_{t\to\infty} V(t)$ exists, then $\lim_{t\to\infty} e_y(t)$ also exists.

Until now, only the convergence of $e_x(t)$ and $\tan(e_\theta(t)/2)$ to 0 has been established. To show the convergence of e_y, at least one of the conditions of Theorem 1 have to be fulfilled. Let us first analyze case 1. Applying Lemma 1 on $\dot{e}_\theta(t)$ ensures that $\lim_{t\to\infty} \dot{e}_\theta(t) = 0$ if $\lim_{t\to\infty} e_\theta(t)$ exists and is finite and $\dot{e}_\theta(t)$ is uniformly continuous. The latter is true [see (9)] if w_b is uniformly continuous. The easiest way to check the uniform continuity of $f(t)$ on $[0,\infty)$ is to see if f, $\dot{f} \in \mathcal{L}_\infty$. The signal w_b defined in (13) is, therefore, uniformly continuous since k_θ and v_r are uniformly continuous from the assumption in case 1 of the theorem. The statement $\lim_{t\to\infty} \dot{e}_\theta(t) = 0$ (which is identical to $\lim_{t\to\infty} w_b(t) = 0$) has therefore been proven. The convergence of e_y to 0 follows from the control law for w_b in (13). The second term in this equation converges to 0 because of $e_\theta \to 2k\pi$ and $k_\theta \in \mathcal{L}_\infty$. It has been shown that w_b converges to 0, and the same is, therefore, true for the first term in the control law for w_b, i.e.,

$$\lim_{t\to\infty} k_y v_r e_y \cos^4\frac{e_\theta}{2} = 0. \tag{21}$$

Taking into account that v_r does not diminish as $t \to \infty$, $\cos^4(e_\theta/2) \to 1$ (which is equivalent to $e_\theta \to 2k\pi$), and $k_y > 0$, (21) can be only satisfied if e_y converges to 0.

For the second case, one has to guarantee again that $\lim_{t\to\infty} w_b = 0$. This is true if v_r and k_θ are uniformly continuous, as shown before. Then Barbãlat's lemma (Lemma 1) is applied on $\dot{e}_x$ in (9). It has been already shown that e_x, e_y, and w_b are uniformly continuous, v_b is uniformly continuous since k_x is uniformly continuous from the assumption of case 2 of the theorem, and w_r is also continuous from the assumption of case 2. This proves the statement $\lim_{t\to\infty} \dot{e}_x(t) = 0$. As previously discussed, it can be concluded that the last two terms in (9) for $\dot{e}_x$ go to 0 as t goes to infinity. Consequently, the product $w_r e_y$ also goes to 0. Since w_r is persistently exciting and does not go to 0, e_y has to go to 0. ■

Remark 1: Note that, for the convergence of e_x and e_θ, only the boundedness of v_r and w_r is required. A considerably more difficult task is to drive e_y to 0. This is achieved by persistent excitation from v_r or w_r. This property is a very general one for the tracking controllers. In fact, it was shown in [9] that no controller is able to achieve asymptotic stability for an arbitrary reference trajectory without persistent excitation, either from v_r or w_r.

Remark 2: It is important to establish the region of attraction of each equilibrium point. Since the convergence of e_y depends on some special conditions, the convergence of e_θ will now be analyzed. It has been already shown [see (20)] that e_θ can never approach $(2k+1)\pi$ if $e_\theta(0) \neq (2k+1)\pi$ $(k \in \mathbb{Z})$. This means that e_θ can never cross any odd multiple of π and that it always converges to $2k\pi$ if the initial condition belongs to the open interval $((2k-1)\pi, (2k+1)\pi)$ where $k \in \mathbb{Z}$. If, however, $e_\theta(0) = (2k+1)\pi$ $(k \in \mathbb{Z})$, it can be easily seen from the control law (13) that $w_b(t) = 0$ and that $e_\theta(t) = (2k+1)\pi$ for $t \geq 0$. This means that the points $e_\theta = (2k+1)\pi$ are unstable equilibrium points (the trajectories are always repelled from them). Even if $e_\theta(t) = (2k+1)\pi$ for $t \geq 0$, as shown above, the translational velocity v becomes $-v_r$ due to (8), which means that the robot is driving in the reverse direction while tracking the desired position without an error. In the case of forward motion robots, such a behavior may sometimes not be acceptable and can be avoided by using an altered control law, as shown in the following.

Remark 3: A useful property of the control law (13) is that it is continuous with respect to the error. The smoothness of control laws is in contradiction with the desire to have a strongly repelling equilibrium point at $e_\theta(t) = (2k+1)\pi$ $(k \in \mathbb{Z})$. If a stronger, but discontinuous, action with respect to the orientation error is needed around the unstable equilibria, this can be achieved by slightly altering the control law (13) as follows:

$$\begin{aligned} v_b &= k_x e_x \\ w_b &= k_y v_r e_y \cos^4\frac{e_\theta}{2} + k_\theta \frac{\sin e_\theta}{\left|\cos\frac{e_\theta}{2}\right|} \\ &= k_y v_r e_y \cos^4\frac{e_\theta}{2} + 2k_\theta \sin\frac{e_\theta}{2}\operatorname{sgn}\left(\cos\frac{e_\theta}{2}\right) \end{aligned} \tag{22}$$

where $\operatorname{sgn}(\cdot)$ is the signum function, and the value of $\operatorname{sgn}(0)$ is defined as either 1 or -1 (actually, anything but 0 to prevent the equilibrium point from arising).

Theorem 2: If the control law (22) is applied to the system (9), where k_y, k_x, k_θ, v_r, and w_r fulfil the same conditions as in Theorem 1, then the tracking error e_x converges to 0, whereas e_θ converges to a multiple of 2π. The convergence of e_y to 0 is guaranteed under the same conditions as in Theorem 1.

Proof: First, the assumption will be made that the initial condition for $e_\theta(t)$ satisfies $\cos(e_\theta(0)/2) \neq 0$. Inserting (22) into (12) yields

$$\dot{V} = -k_x k_y e_x^2 - 4k_\theta \frac{\tan^2 \frac{e_\theta}{2}}{\left|\cos \frac{e_\theta}{2}\right|} \tag{23}$$

which results in the fulfillment of (15) and (16) as before and in e_x, $|\cos(e_\theta/2)|^{-(1/2)} \tan(e_\theta/2) \in \mathcal{L}_2$. From $|\cos(e_\theta/2)|^{-(1/2)} \tan(e_\theta/2) \geq \tan(e_\theta/2)$ it follows that $\tan(e_\theta/2) \in \mathcal{L}_2$. As previously discussed, the convergence of e_x and $\tan(e_\theta/2)$ to 0 can be concluded. The proof of the convergence of e_y follows the same lines as the proof of Theorem 1.

As already shown in the proof of Theorem 1, $e_\theta(t)$ never crosses $(2k+1)\pi$ if $\cos(e_\theta(0)/2) \neq 0$. If $\cos(e_\theta(0)/2) = 0$, the initial value of the control (22) becomes

$$w_b(0) = 2k_\theta(0) \sin \frac{e_\theta(0)}{2} \tag{24}$$

where it was taken into account that $\operatorname{sgn}(0) = 1$. This means that $w_b(0) > 0$ and that e_θ will start to rapidly decrease if $e_\theta(0) \in \{\ldots, -3\pi, \pi, 5\pi, \ldots\}$ and $w_b(0) < 0$, and e_θ will start to rapidly increase if $e_\theta(0) \in \{\ldots, -5\pi, -\pi, 3\pi, \ldots\}$. When e_θ leaves this undesirable orientation, it is impossible to visit it again, and the convergence of e_θ to $2k\pi$ $(k \in \mathbb{Z})$ follows. ■

Remark 4: Note that the discontinuity in the control law at $e_\theta(t) = (2k+1)\pi$ $(k \in \mathbb{Z})$ does not influence the uniform continuity of any signal involved in the system. As already shown in the proof of Theorem 1, $e_\theta(t)$ never crosses $(2k+1)\pi$ if $\cos(e_\theta(0)/2) \neq 0$. If $\cos(e_\theta(0)/2) = 0$, the initial value of all the signals in the system is finite. The signals also remain smooth later.

B. Unified Framework for Control Laws Analysis and Design

One of the major advantages of this paper is that it proposes a unified framework for a control law stability analysis. Within this framework, the design of new control laws is also possible. A general form of the Lyapunov function (11) will be used, i.e.,

$$V = \frac{k_y}{2}\left(e_x^2 + e_y^2\right) + V_1(e_\theta) \tag{25}$$

where k_y is a positive constant, and $V_1 : \mathbb{R} \to \mathbb{R}$ is a periodic function (the period is 2π) that is positive everywhere, except at multiples of 2π, where it becomes 0. Its derivative along the solutions of (9) is

$$\dot{V} = -k_y e_x v_b + k_y v_r e_y \sin e_\theta - w_b \frac{dV_1}{de_\theta}. \tag{26}$$

Now v_b and w_b have to be found to make the derivative negative. The control law for v_b will make the first term quadratically negative with respect to e_x; w_b will cancel the second term on the right-hand side of (26) and make the last one negative with respect to e_θ (the third term will become 0 at multiples of 2π). The general form of the control laws that unify all the laws treated in this paper is the following:

$$\begin{aligned} v_b &= k_x e_x \\ w_b &= k_y v_r e_y \Omega_y(e_\theta) + k_\theta \Omega_\theta(e_\theta) \end{aligned} \tag{27}$$

where k_x and k_θ are positive bounded functions, whereas $\Omega_y(e_\theta)$ and $\Omega_\theta(e_\theta)$ need to be defined. Inserting (27) into (26), the following is obtained:

$$\dot{V} = -k_y k_x e_x^2 + k_y v_r e_y \left(\sin e_\theta - \Omega_y \frac{dV_1}{de_\theta}\right) - k_\theta \Omega_\theta \frac{dV_1}{de_\theta}. \tag{28}$$

The convergence of e_x to 0 and the convergence of e_θ to any multiple of 2π is guaranteed if both conditions are met, i.e.,

$$\sin e_\theta - \Omega_y \frac{dV_1}{de_\theta} = 0 \tag{29}$$

$$k_\theta \Omega_\theta \frac{dV_1}{de_\theta} \begin{cases} = 0, & e_\theta = 2k\pi \quad (k \in \mathbb{R}) \\ > 0, & \text{elsewhere.} \end{cases} \tag{30}$$

It is very important that the expression $k_\theta \Omega_\theta (dV_1/de_\theta)$ is locally quadratically positive around the zeros to guarantee the convergence of e_θ.

It is simple to check that the functions $\Omega_y(e_\theta)$ and $\Omega_\theta(e_\theta)$ are continuous for the case of (13), whereas the discontinuity occurs at $e_\theta = \pm\pi$ for the case of (22). The shape of the functions for different control laws is shown in Fig. 2. As already stated, this discontinuity is introduced to prevent the occurrence of an unstable equilibrium. The control laws defined by (13) and (22), respectively, guarantee the convergence of all the errors to 0 if both reference velocities do not diminish. Both control laws share the $\Omega_y(e_\theta)$ function and differ in $\Omega_\theta(e_\theta)$. It is very easy to show that the linear combination of the two proposed control laws

$$\begin{aligned} v_b &= k_x e_x \\ w_b &= k_y v_r e_y \cos^4 \frac{e_\theta}{2} + c k_\theta \sin e_\theta \\ &\quad + (1-c) 2k_\theta \sin \frac{e_\theta}{2} \operatorname{sgn}\left(\cos \frac{e_\theta}{2}\right) \end{aligned} \tag{31}$$

also guarantees convergence under the same conditions, where $0 \leq c \leq 1$ is an arbitrary real constant. By tuning c, the size of the discontinuity at $e_\theta = \pm\pi$ is influenced ($c = 0$ for the maximum discontinuity; $c = 1$ for the continuous control law). By selecting c smaller than 1, the occurrence of the unstable equilibrium is prevented.

Note that the actual control v can become negative during transients. This would mean that the robot would have to drive backward for a short period of time. If this is not allowed, the control v is simply limited to 0 from below, and only rotation takes part for a short period of time. When the robot's orientation changes enough, the control v becomes positive again, and the forward motion automatically continues, as will be shown in Section V.

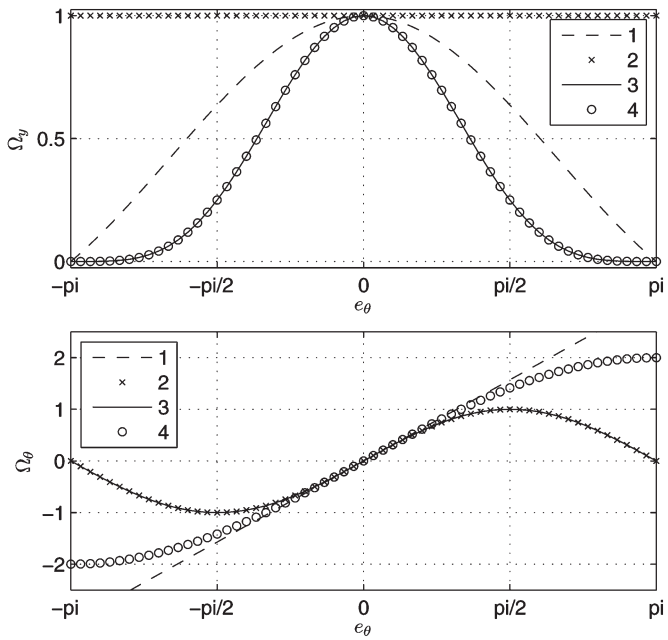

Fig. 2. Shape of $\Omega_y(e_\theta)$ and $\Omega_\theta(e_\theta)$ in the control laws for forward motion robots (indices 1–4 correspond to those in Table I).

Two known control laws from the literature can be also analyzed in the proposed framework. The first one is from [11], and the other one is from [14]. These algorithms were chosen because they were both designed using the Lyapunov stability theory. The Lyapunov functions used therein have the same limit around the zero error in the orientation $(e_\theta = 0)$. Choosing the Lyapunov function as

$$V = \frac{k_y}{2}\left(e_x^2 + e_y^2\right) + \frac{1}{2}\left(\frac{\sin\frac{e_\theta}{2}}{\frac{1}{2}}\right)^2 \tag{32}$$

and using the control law proposed in [11], i.e.,

$$\begin{aligned} v_b &= k_x e_x \\ w_b &= k v_r e_y + k_\theta \sin e_\theta \end{aligned} \tag{33}$$

result in a stable system where the convergence of all the errors can be shown under the same conditions as in Theorems 1 and 2. Note that there was also a third factor $|v_r|$ in the second term of w_b, which can be also included in k_θ.

If one chooses the Lyapunov function

$$V = \frac{k_y}{2}\left(e_x^2 + e_y^2\right) + \frac{1}{2}e_\theta^2 \tag{34}$$

and implements the feedback control law from [14], i.e.,

$$\begin{aligned} v_b &= k_x e_x \\ w_b &= k v_r e_y \frac{\sin e_\theta}{e_\theta} + k_\theta e_\theta \end{aligned} \tag{35}$$

the same conditions for the convergence can again be derived. Note that the control law (35) is not completely compatible with the proposed approach since it is not periodic with respect to e_θ, but in this paper, it will be only analyzed in the interval $(-\pi, \pi)$.

C. Forward and Backward Motion Control of Wheeled Mobile Robots

As aforementioned, the forward and backward motion robot in our context means that the robot can be driven in both directions not only during transients but also during normal behavior. When controlling such a vehicle, our goal is to bring the position error to zero, whereas the orientation error should converge to any multiple of π (even multiples of π for the forward motion and odd multiples of π for the backward motion). The Lyapunov function should be therefore periodic with respect to e_θ with a period of π. The Lyapunov functions will have the same form as (25), but the period of V_1 will be π instead of 2π. The same form of control laws (27) will be used, resulting in the same derivative of the Lyapunov function (28). This means that the same stability conditions are obtained, i.e., (29) and (30), where the period of $k_\theta \Omega_\theta (dV_1/de_\theta)$ is now π, i.e.,

$$k_\theta \Omega_\theta \frac{dV_1}{de_\theta} \begin{cases} = 0, & e_\theta = k\pi \quad (k \in \mathbb{R}) \\ < 0, & \text{elsewhere.} \end{cases} \tag{36}$$

Obviously, the period of Ω_θ also becomes π.

The conditions (29) and (36) enable a wide spectrum of control laws to be developed. Some will be shown here, and their properties will be compared in Section IV. The first Lyapunov function candidate, which is inspired by (11), is chosen as

$$V = \frac{k_y}{2}\left(e_x^2 + e_y^2\right) + \frac{1}{2}\tan^2 e_\theta. \tag{37}$$

Analogously to the approach in the previous subsection, the control law will be derived such that it results in a derivative of the Lyapunov function of the following form [analogous to (14)]:

$$\dot{V} = -k_x k_y e_x^2 - k_\theta \tan^2 e_\theta. \tag{38}$$

It is very easy to show that the required feedback controls are

$$\begin{aligned} v_b &= k_x e_x \\ w_b &= k_y v_r e_y \cos^3 e_\theta + k_\theta \frac{\sin 2e_\theta}{2}. \end{aligned} \tag{39}$$

Theorem 3: If the control law (39) is applied to the system where k_y is a positive constant, k_x and k_θ are positive bounded functions, the reference velocities v_r and w_r are bounded, and the initial condition for $e_\theta(t)$ satisfies $\cos e_\theta(0) \neq 0$, then the tracking error e_x converges to 0, whereas e_θ converges to a multiple of π. The convergence of e_y to 0 is guaranteed, provided that at least one of the two conditions of Theorem 1 is satisfied.

Proof: The proof is completely analogous to the proof of Theorem 1.

The next Lyapunov function is analogous to (32), i.e.,

$$V = \frac{k_y}{2}\left(e_x^2 + e_y^2\right) + \frac{1}{2}\sin^2 e_\theta. \tag{40}$$

Unfortunately, no w_b exists that would remain bounded if $\cos e_\theta$ approached 0. The Lyapunov function should be therefore slightly modified in view of condition (36), i.e.,

$$V = \frac{k_y}{2}\left(e_x^2 + e_y^2\right) + \frac{1}{2}\sin^2 e_\theta \left|\cos(e_\theta)\right|^{-1}. \tag{41}$$

The following form of the Lyapunov function derivative

$$\dot{V} = -k_x k_y e_x^2 - k_\theta \sin^2 e_\theta \left|\cos(e_\theta)\right| \tag{42}$$

is obtained by using the control law (27) and choosing Ω_y and Ω_θ as

$$\Omega_y(e_\theta) = \left(1 + \frac{\tan^2 e_\theta}{2}\right)^{-1} \operatorname{sgn}(\cos e_\theta)$$
$$\Omega_\theta(e_\theta) = \left(1 + \frac{\tan^2 e_\theta}{2}\right)^{-1} \frac{\sin 2e_\theta}{2}. \tag{43}$$

The proposed framework allows the same Lyapunov function (41) to be used, and a different $\dot{V}$ is required because of the inequality in (36), i.e.,

$$\dot{V} = -k_x k_y e_x^2 - k_\theta \sin^2 e_\theta \left|\cos(e_\theta)\right| \left(1 + \frac{\tan^2 e_\theta}{2}\right). \tag{44}$$

This results in the same Ω_y due to (29) and a simpler form of Ω_θ due to (36), i.e.,

$$\Omega_y(e_\theta) = \left(1 + \frac{\tan^2 e_\theta}{2}\right)^{-1} \operatorname{sgn}(\cos e_\theta)$$
$$\Omega_\theta(e_\theta) = \frac{\sin 2e_\theta}{2}. \tag{45}$$

For both the control laws (43) and (45), the convergence can be proven under the same conditions as in Theorem 3.

The advantage of the control laws (39), (43), and (45) is that they are continuous, which results in continuous (kinematic) control signals. Continuous kinematic controls make the problem of implementation on the vehicle with dynamics much easier. The drawback of the control laws (39), (43), and (45) is their inability to drive the errors to 0 if $\cos e_\theta(0) = 0$. This condition is satisfied if, e.g., $e_\theta(0) = (\pi/2)$. It is easy to see that, in such a case, w_b will be 0 in all three cases. Again, a problem of unstable equilibrium can be recognized where $\cos e_\theta = 0$. The source of the problems lies in the fact that the Lyapunov function becomes unbounded where $\cos e_\theta = 0$. This can be resolved if a modified Lyapunov function is used, i.e.,

$$V = \frac{k_y}{2}\left(e_x^2 + e_y^2\right) + \frac{1}{2}\sin^2 e_\theta \frac{a+1}{a + |\cos(e_\theta)|} \tag{46}$$

where $a \geq 0$ is an arbitrary constant, and $(a+1)$ in the numerator is only used to have the same behavior of V around zero error as in the other control laws treated in this paper. Again, several control laws can be proposed that guarantee the convergence of the tracking error to 0. The following form of $\dot{V}$:

$$\dot{V} = -k_x k_y e_x^2 - k_\theta \sin^2 e_\theta \tag{47}$$

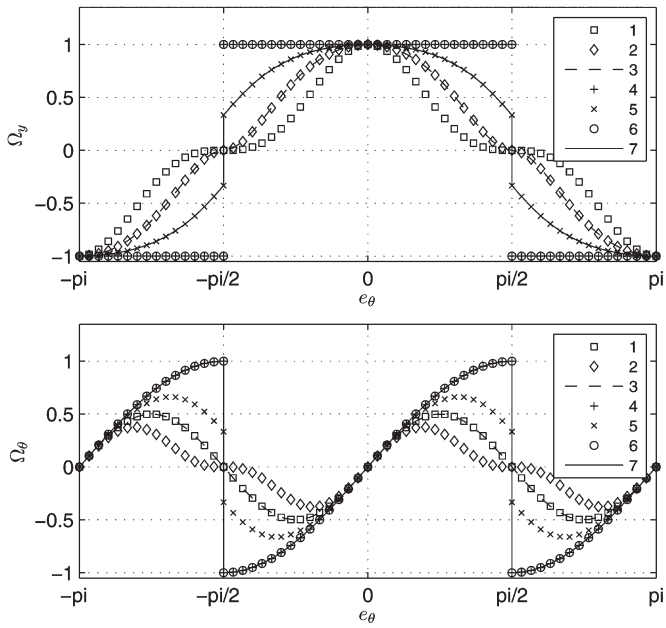

Fig. 3. Shape of $\Omega_y(e_\theta)$ and $\Omega_\theta(e_\theta)$ in the control laws for forward and backward motion (indices 1–7 correspond to those in Table II).

is obtained when applying the control law with the following Ω functions:

$$\Omega_y(e_\theta) = \frac{2}{a+1}\operatorname{sgn}(\cos e_\theta)\left(1 + \frac{1-a^2}{(a+|\cos e_\theta|)^2}\right)^{-1}$$
$$\Omega_\theta(e_\theta) = \frac{2}{a+1}\operatorname{sgn}(\cos e_\theta)\left(1 + \frac{1-a^2}{(a+|\cos e_\theta|)^2}\right)^{-1}\sin e_\theta. \tag{48}$$

The functions from (48) are continuous everywhere, except at odd multiples of $\pi/2$. After a simple check, it can be concluded that the functions can be made continuous by choosing a equal to 0, whereas the size of the jumps increases by increasing a. A simple form is obtained at $a = 1$ when Ω_y becomes $\operatorname{sgn}(\cos e_\theta)$. By increasing a further, the control signals may become very large in the vicinity of $\pm(\pi/2)$.

The last control law can be obtained by requiring $\dot{V}$ to take the following form:

$$\dot{V} = -k_x k_y e_x^2 - k_\theta \frac{a+1}{2}\left(1 + \frac{1-a^2}{(a+|\cos e_\theta|)^2}\right)\sin^2 e_\theta \tag{49}$$

which results in a simpler control law with the following Ω functions:

$$\Omega_y(e_\theta) = \frac{2}{a+1}\operatorname{sgn}(\cos e_\theta)\left(1 + \frac{1-a^2}{(a+|\cos e_\theta|)^2}\right)^{-1}$$
$$\Omega_\theta(e_\theta) = \operatorname{sgn}(\cos e_\theta)\sin e_\theta. \tag{50}$$

All the Ω functions for forward and backward motion control of the wheeled mobile robots are summarized in Table II and Fig. 3, where $\beta_a(e_\theta)$ stands for

$$\beta_a(e_\theta) = \frac{2}{a+1}\operatorname{sgn}(\cos e_\theta)\left(1 + \frac{1-a^2}{(a+|\cos e_\theta|)^2}\right)^{-1}. \tag{51}$$

Remark 5: The convergence proofs for the control laws here are very similar to the ones from the previous subsection and are omitted.

IV. Comparison of Different Control Laws

The proposed control laws were extensively tested and compared with the existing methods from the literature given by (33) and (35). Note that all the control laws treated in this paper behave similarly around the zero orientation error, which can be shown by analyzing the Ω functions around 0, i.e.,

$$\Omega_y\Big|_{e_\theta=0}=1 \qquad \frac{d\Omega_y}{de_\theta}\Big|_{e_\theta=0}=0$$
$$\Omega_\theta\Big|_{e_\theta=0}=0 \qquad \frac{d\Omega_\theta}{de_\theta}\Big|_{e_\theta=0}=1. \tag{52}$$

This will enable a relatively fair comparison among the control laws by using the same control gains—in all cases, the values $k_x = 10\ \mathrm{s}^{-1}$, $k_y = 10\ \mathrm{m}^{-2}$, and $k_\theta = 1\ \mathrm{s}^{-1}$ will be used. In the simulation experiments, the orientation error e_θ for the nonperiodic control law (35) was always mapped to the interval $(-\pi, \pi]$ to make the comparison fair.

The form of the control laws suggests that the role of v_b is always the reduction of e_x while w_b needs to cater for the remaining two errors. A very simplified explanation is that the first term in w_b takes care of the lateral error while the second term is responsible for the orientation error. In reality, the problems are much more complicated due to the nonholonomic nature of the system. The feedback v_b is the same in all the control laws that were compared, and therefore, any drastic differences in performance should not be expected. The form of w_b suggested by (27) is also the same for all the control laws. The shape of the Ω functions, however, drastically changes. Some control laws are continuous with respect to the orientation error (which is a useful property but causes the occurrence of unstable equilibria), the others are not. In addition, the "gains" from e_y and e_θ, respectively, to w_b are very different (although they are the same in the nominal operating point).

An extensive simulation study was performed to compare all the approaches under the same circumstances. The reference trajectory is the same in all the simulation runs, i.e.,

$$x_r(t) = A_0\cos(\omega_0 t)$$
$$y_r(t) = A_0\sin(2\omega_0 t) \tag{53}$$

with $A_0 = 1$ m, and $\omega_0 = 0.34\ \mathrm{s}^{-1}$. The simulation run always started at $t = 0$ and finished at $t = (2\pi/\omega_0)$. The control signals v_b and w_b were saturated to ± 10 (ms^{-1} and s^{-1}, respectively). The simulation experiment was conducted with different initial conditions. The possible initial conditions of the error model were

$$\frac{e_x(0)}{A_0}, \frac{e_y(0)}{A_0} \in I_{xy} = \{-1.9, -1.7, -1.5, \ldots, 1.7, 1.9\}$$
$$e_\theta(0) \in I_\theta = \left\{ -\pi + \frac{\pi}{24} + \frac{l\pi}{12} \,\middle|\, l = 0, 1, \ldots, 23 \right\} \tag{54}$$

TABLE I
The Form of $\Omega_y(e_\theta)$ and $\Omega_\theta(e_\theta)$ in the Control Laws for Forward Motion Robots (the Indices Are the Same as in Fig. 2)

index	Eq. Nr.	$\Omega_y(e_\theta)$	$\Omega_\theta(e_\theta)$
1	(35) [14]	$\frac{\sin e_\theta}{e_\theta}$	e_θ
2	(33) [11]	1	$\sin e_\theta$
3	(13)	$\cos^4\frac{e_\theta}{2}$	$\sin e_\theta$
4	(22)	$\cos^4\frac{e_\theta}{2}$	$\sin\frac{e_\theta}{2}\,\mathrm{sgn}\left(\cos\frac{e_\theta}{2}\right)$

TABLE II
The Form of $\Omega_y(e_\theta)$ and $\Omega_\theta(e_\theta)$ in the Control Laws for Forward and Backward Motion (the Indices Are the Same as in Fig. 3)

index	Eq. Nr.	$\Omega_y(e_\theta)$	$\Omega_\theta(e_\theta)$
1	(39)	$\cos^3 e_\theta$	$\frac{\sin 2e_\theta}{2}$
2	(43)	$\frac{\mathrm{sgn}(\cos e_\theta)}{1+\frac{\tan^2 e_\theta}{2}}$	$\frac{\frac{\sin 2e_\theta}{2}}{1+\frac{\tan^2 e_\theta}{2}}$
3	(45)	$\frac{\mathrm{sgn}(\cos e_\theta)}{1+\frac{\tan^2 e_\theta}{2}}$	$\frac{\sin 2e_\theta}{2}$
4	(48)	$\beta_1(e_\theta)$	$\beta_1(e_\theta)\sin e_\theta$
5	(48)	$\beta_{0.5}(e_\theta)$	$\beta_{0.5}(e_\theta)\sin e_\theta$
6	(50)	$\beta_1(e_\theta)$	$\mathrm{sgn}(\cos e_\theta)\sin e_\theta$
7	(50)	$\beta_{0.5}(e_\theta)$	$\mathrm{sgn}(\cos e_\theta)\sin e_\theta$

which means that each of the proposed control laws has been tested with all the variations of the initial conditions from the grid (54). For each simulation run, the following error functions were calculated:

$${}^i c_p^{xy\theta} = \int_0^{\frac{2\pi}{\omega_0}} \left[e_x^2(t) + e_y^2(t)\right] dt$$
$${}^i c_o^{xy\theta} = \int_0^{\frac{2\pi}{\omega_0}} \left[e_\theta^2(t)\right] dt \tag{55}$$

where the indexes "p" and "o" stand for the position and the orientation error, respectively; x, y, and θ denote the respective initial conditions; and i denotes the index of the control law. Eleven different control laws were tested: four for the forward motion robots (they are summarized in Table I) and seven for the forward and backward motion robots (they are summarized in Table II). For each variation of the initial conditions in (54), eleven simulation experiments were conducted with eleven different control laws, meaning that the total number of simulation runs was $20 \times 20 \times 24 \times 11$.

The overall cost function of a certain control law i was simply the sum of all the individual cost functions, i.e.,

$$C_p^i = \sum_{x\in I_{xy}}\sum_{y\in I_{xy}}\sum_{\theta\in I_\theta}\left({}^i c_p^{xy\theta}\right)$$
$$C_o^i = \sum_{x\in I_{xy}}\sum_{y\in I_{xy}}\sum_{\theta\in I_\theta}\left({}^i c_o^{xy\theta}\right). \tag{56}$$

Whenever the performance of a control law is discussed, it is necessary to check for the control effort. Analogously with (55) and (56), C_v^i and C_w^i are defined as the sums of the integrals of v_b^2 and w_b^2, respectively. Table III shows the cost functions $\overline{C}_p^i$, $\overline{C}_o^i$, $\overline{C}_v^i$, and $\overline{C}_w^i$ (these are obtained by normalizing the

TABLE III
COST FUNCTIONS OF INDIVIDUAL CONTROL LAWS FOR THE FORWARD MOTION CONTROL LAWS

i	$\overline{C}_p^i$	$\overline{C}_o^i$	$\overline{C}_v^i$	$\overline{C}_w^i$
1	1.7315	1.2805	1.0096	1.2567
2	1	1.1574	1.2134	2.2762
3	2.6368	1.6913	1.0238	1.0056
4	1.9060	1	1	1

TABLE IV
COST FUNCTIONS OF INDIVIDUAL CONTROL LAWS FOR THE FORWARD AND BACKWARD MOTION CONTROL LAWS

i	$\overline{C}_p^i$	$\overline{C}_o^i$	$\overline{C}_v^i$	$\overline{C}_w^i$
1	1.5802	1	1	1
2	2.1642	2.9317	1.2868	2.3856
3	1.1796	1.4556	1.0018	1.4684
4	1.2243	2.0122	1.1401	2.4733
5	1.2847	2.1131	1.1323	2.1756
6	1.2243	2.0122	1.1401	2.4733
7	1	1.4242	1.0302	1.7277

respective cost functions with the best one in the column) for all the forward motion control laws from Table I. Similarly, Table IV shows the cost functions for all the forward and backward motion control laws from Table II.

Among the forward motion control laws, the smallest position error C_p^i (or $\overline{C}_p^i$) is achieved with the control law (33), whereas the smallest orientation error and the smallest control effort (both in translational and angular velocities) is achieved by the proposed control law (22). Similar results were obtained when testing the forward and backward motion control laws, where the best overall performance in the position error is achieved with the control law (50), whereas the control law (39) achieves the best results in the other categories.

It is very well known that it is impossible to simultaneously drive the lateral and orientation errors to 0 independently due to the nonholonomic nature of the system. This means that there is always some tradeoff between good position control and good orientation control. In our approach, this can be done in two ways—by properly choosing the control gains and by suitably selecting the control law. By choosing a large k_θ, the main control goal is to reduce the error in the orientation, whereas the lateral error is not so important. Such a strategy is useful when the error in the orientation is high and it is necessary to reduce it quite quickly (otherwise, the error in e_y can also increase due to the interconnection). When, on the other hand, the orientation error is low, it is more important to cope with e_y, which is a problematic error due to the nonholonomic constraints. Such behavior is achieved by selecting a control law with a narrow Ω_y (narrow means that $|\Omega_y|$ is around 1 for very small angles and that it starts converging to 0 for relatively small values of $|e_\theta|$, whereas wide means that $|\Omega_y|$ is closer to 1 even when $|e_\theta|$ approaches $\pi/2$) function and discontinuous Ω_θ, which is the case with the fourth control law from Table I and the seventh control law from Table II.

V. HARDWARE IMPLEMENTATION

The algorithms were validated using the Mirosot-type robot soccer robot, observed with one firewire camera, mounted above the flat uniformly lit surface, at 30 frames per second. A custom-developed computer-vision system was used to determine the position and the orientation of the robot in each captured video frame and publish this information as a publishing node to the Robot Operating System (ROS). Commands to the robot were wirelessly sent from the second ROS node, whereas a third ROS node was used to execute the control algorithms. All the nodes were executed on the same computer.

The practical implementation validated the proposed control laws in a real-life environment where the system is subject to conditions not explicitly taken into account during the control law development. The schematic representation of the system is given in Fig. 4. Not only does a real robot introduce dynamics to the control problem, its pose measurement is also delayed due to the machine vision measurement. Consequently, the commands v and w are transformed to the velocity references of the wheels v_R and v_L, as suggested by (3), whereas PID controllers are implemented on board to force that the actual wheel velocities v_R^a and v_L^a track the reference velocities fast enough. The low-level PID-controlled loop was identified as a first-order system with 150-ms time constant due to the robot dynamics. The total delay of 50 ms due to video capture, processing, interprocess communication, control algorithms' evaluation, and wireless communication to the robots was experimentally estimated. It is very well known that parasitic dynamics and delays in the loop decrease the phase margin and can eventually cause system instability. However, experimental results have confirmed that the stability margin of the proposed control laws is high enough to prevent performance degradation due to unmodelled dynamics.

The experimental results show very good tracking performance in the case of all the proposed control laws if the robot is near the reference trajectory and if the control gains are not too high. The differences are notable in the transient (when the control errors are relatively high). Probably the most problematic initial pose is when the robot's initial orientation is perpendicular to the initial trajectory and the robot is turned away from the trajectory. This case is treated in the experiments, whose results are shown in Figs. 5–7. Since some controllers produce similar results, not all of them are included in the plots to improve the legibility. The figures show the results of the experiments for the reference trajectory (53) and the control gains $k_x = 2$, $k_y = 5$, and $k_\theta = 0.8$. Only the most distinct controllers are depicted—controller 3 from Table I (blue narrow solid lines) and controllers 2, 4, and 7 from Table II (dashed lines). They are compared with the controllers from the literature (II-1 and II-2, red and green thicker solid lines) and to a linear controller $v_b = k_x e_x$ and $w_b = k_y e_y + k_\theta e_\theta$ (magenta dash-dotted line). In the case of the forward-motion-only controllers, the v command was limited to 0 from below (reverse driving is not possible). The results of the forward-motion-only controllers (group I) are shown with a solid line, whereas the results of group II are shown with a dashed line. In the group of forward and backward motion robots, one robot is driving in the forward direction after the transient, whereas two are driving backward (this is why the "error" in the orientation is $-\pi$ in the steady state). In group II, controller II-2 behaves the worst due to the particular initial condition in

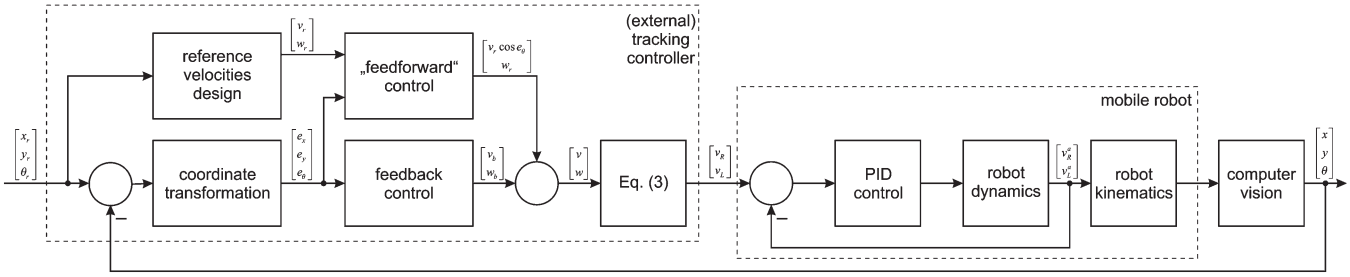

Fig. 4. Schematic of the system.

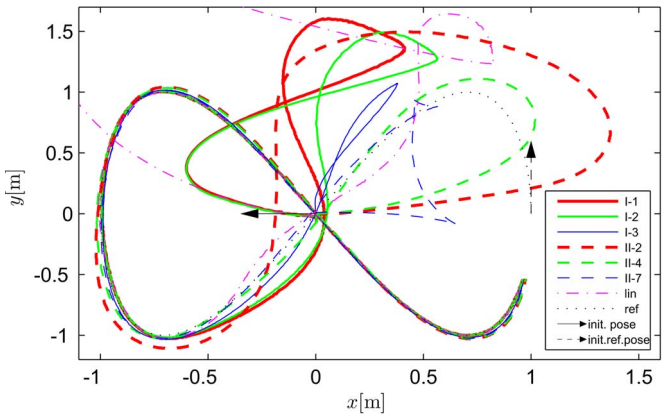

Fig. 5. Trajectories in the $x-y$ plane.

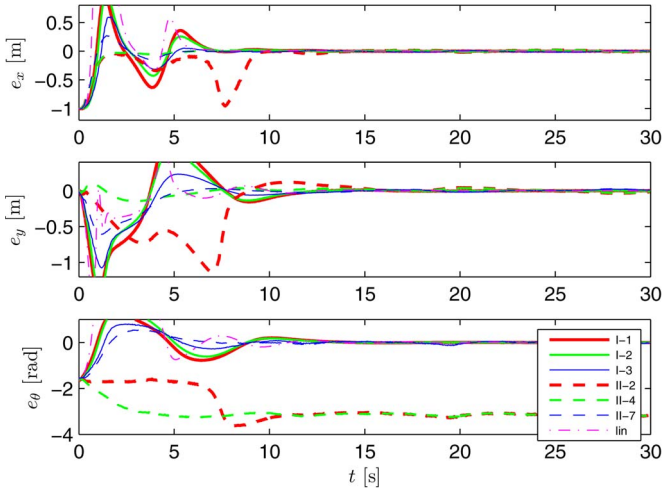

Fig. 6. Error signals.

the vicinity of the weakly repelling equilibrium of $-(\pi/2)$ (see the orientation error). The comparison shows quite different transients, although all the controllers (except the linear one) behave exactly the same around the zero error. The control gains are not optimized for each individual controller because this would have to be done for each reference trajectory. This is why these results should not be seen as a measure of the "quality" of the controllers but rather to show the diversity and the ability of the controllers to cope with real problems, even in the case of bad initial conditions.

Extensive tests have shown that the controllers from Table I result in the trajectories that are relatively similar to each other, whereas the group of controllers from Table II shows

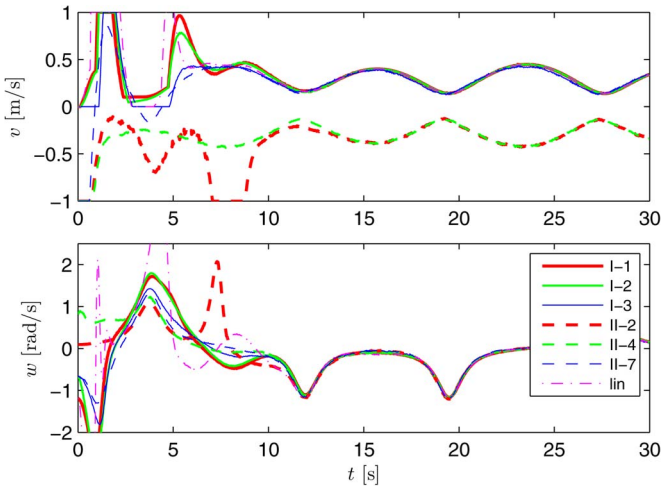

Fig. 7. Control signals.

much more heterogeneous behavior, as shown in Figs. 5–7. The control laws with a discontinuity in Ω_θ around $\pm 90^\circ$ generally produce better results since the orientation error is quickly repelled from this unfavorable value, but the control cost is a little higher. Controller II-7 is a good overall performer and can be recommended for use in practice.

VI. Conclusion

In this paper, a set of control laws has been developed, which are periodic with respect to the orientation error. They are divided into two categories—the laws for forward motion mobile robots and the laws for forward and backward motion mobile robots. All the laws are derived within the Lyapunov stability framework, and global asymptotic convergence to a predesigned path is proven under some mild conditions if the reference velocities satisfy the condition of persistent excitation. The control laws are also discussed from the continuity point of view, which is often in contradiction with the absence of unstable equilibria for a certain orientation error. Another important tradeoff is also discussed—how to achieve good position regulation and good orientation regulation. This can be done by properly choosing the control gains and by suitably selecting one of the proposed control laws. The proposed control laws are also very easy to implement on low-cost hardware since they require only basic mathematical operations and trigonometric functions. Moreover, due to the periodicity of control laws, no special treatment of cases when orientation error exceeds $\pm 180^\circ$ is necessary.

REFERENCES

[1] Z. Wang and D. Gu, "Cooperative target tracking control of multiple robots," *IEEE Trans. Ind. Electron.*, vol. 59, no. 8, pp. 3232–3240, Aug. 2012.

[2] D. Buccieri, D. Perritaz, P. Mullhaupt, Z.-P. Jiang, and D. Bonvin, "Velocity-scheduling control for a unicycle mobile robot: Theory and experiments," *IEEE Trans. Robot.*, vol. 25, no. 2, pp. 451–458, Apr. 2009.

[3] Y. Toda and N. Kubota, "Self-localization based on multiresolution map for remote control of multiple mobile robots," *IEEE Trans. Ind. Informat.*, vol. 9, no. 3, pp. 1772–1781, Aug. 2013.

[4] J.-X. Xu, Z.-Q. Guo, and T. H. Lee, "Design and implementation of a Takagi–Sugeno-type fuzzy logic controller on a two-wheeled mobile robot," *IEEE Trans. Ind. Electron.*, vol. 60, no. 12, pp. 5717–5728, Dec. 2013.

[5] S. J. Kim and B. K. Kim, "Dynamic ultrasonic hybrid localization system for indoor mobile robots," *IEEE Trans. Ind. Electron.*, vol. 60, no. 10, pp. 4562–4573, Oct. 2013.

[6] Z.-P. Jiang and H. Nijmeijer, "Tracking control of mobile robots: A case study in backstepping," *Automatica*, vol. 33, no. 7, pp. 1393–1399, Jul. 1997.

[7] R. W. Brockett, *Differential Geometric Control Theory*. Boston, MA, USA: Birkhauser, 1983, ch. Asymptotic stability and feedback stabilization, pp. 181–191.

[8] P. Morin and C. Samson, "Control of nonholonomic mobile robots based on the transverse function approach," *IEEE Trans. Robot.*, vol. 25, no. 5, pp. 1058–1073, Oct. 2009.

[9] D. Lizarraga, "Obstructions to the existence of universal stabilizers for smooth control systems," *Math. Control, Signals Syst.*, vol. 16, no. 4, pp. 255–277, Mar. 2004.

[10] F. Pourboghrat, "Exponential stabilization of nonholonomic mobile robots," *Comput. Electr. Eng.*, vol. 28, no. 5, pp. 349–359, 2002.

[11] Y. Kanayama, Y. Kimura, F. Miyazaki, and T. Noguchi, "A stable tracking control method for an autonomous mobile robot," in *Proc. IEEE Int. Conf. Robot. Autom.*, Los Alamitos, CA, USA, 1990, vol. 1, pp. 384–389.

[12] C. Pozna, F. Troester, R.-E. Precup, J. K. Tar, and S. Preitl, "On the design of an obstacle avoiding trajectory: Method and simulation," *Math. Comput. Simul.*, vol. 79, no. 7, pp. 2211–2226, Mar. 2009.

[13] G. Klančar, D. Matko, and S. Blažič, "A control strategy for platoons of differential drive wheeled mobile robot," *Robot. Auton. Syst.*, vol. 59, no. 2, pp. 57–64, Feb. 2011.

[14] C. Samson, "Time-varying feedback stabilization of car like wheeled mobile robot," *Int. J. Robot. Res.*, vol. 12, no. 1, pp. 55–64, Feb. 1993.

[15] S. Blažič, "A novel trajectory-tracking control law for wheeled mobile robots," *Robot. Auton. Syst.*, vol. 59, no. 11, pp. 1001–1007, Nov. 2011.

[16] G. Klančar and I. Škrjanc, "Tracking-error model-based predictive control for mobile robots in real time," *Robot. Auton. Syst.*, vol. 55, no. 6, pp. 460–469, Jun. 2007.

[17] E.-H. Guechi, J. Lauber, M. Dambrine, G. Klančar, and S. Blažič, "PDC control design for non-holonomic wheeled mobile robots with delayed outputs," *J. Intell. Robot. Syst.*, vol. 60, no. 3, pp. 395–414, Dec. 2010.

[18] R.-E. Precup, R.-C. David, E. Petriu, S. Preitl, and M.-B. Radac, "Fuzzy control systems with reduced parametric sensitivity based on simulated annealing," *IEEE Trans. Ind. Electron.*, vol. 59, no. 8, pp. 3049–3061, Aug. 2012.

[19] Y. Fang, X. Liu, and X. Zhang, "Adaptive active visual servoing of nonholonomic mobile robots," *IEEE Trans. Ind. Electron.*, vol. 59, no. 1, pp. 486–497, Jan. 2012.

[20] C.-Y. Chang and H. Wijaya Lie, "Real-time visual tracking and measurement to control fast dynamics of overhead cranes," *IEEE Trans. Ind. Electron.*, vol. 59, no. 3, pp. 1640–1649, Mar. 2012.

[21] R.-E. Precup and H. Hellendoorn, "A survey on industrial applications of fuzzy control," *Comput. Ind.*, vol. 62, no. 3, pp. 213–226, Apr. 2011.

[22] R. C. Coulter, "Implementation of the pure pursuit path tracking algorithm," Robotics Inst., Carnegie Mellon Univ., Pittsburgh, PA, USA, Rep. CMU-RI-TR-92-01, 1992.

[23] P. A. Ioannou and J. Sun, *Robust Adaptive Control*. Englewood Cliffs, NJ, USA: Prentice-Hall, 1996.

Sašo Blažič received B.Sc., M.Sc., and Ph.D. degrees from the University of Ljubljana, Ljubljana, Slovenia, in 1996, 1999, and 2002, respectively.

He is currently an Associate Professor with the University of Ljubljana. His research interests include adaptive, fuzzy, and predictive control of dynamical systems and modeling of nonlinear systems, as well as, lately, the areas of autonomous mobile systems and satellite systems.